

A Photochemical Method for Patterning the Immobilization of Ligands and Cells to Self-Assembled Monolayers

W. Shannon Dillmore,[†] Muhammad N. Yousaf,[†] and Milan Mrksich*

Department of Chemistry, The University of Chicago, 5735 S. Ellis Avenue, Chicago, Illinois 60637

Received January 19, 2004. In Final Form: June 7, 2004

This work describes a chemically well defined method for patterning ligands to self-assembled monolayers (SAMs) of alkanethiolates on gold. This method begins with monolayers presenting a nitroveratryloxy-carbonyl (NVOC)-protected hydroquinone which is photochemically irradiated to reveal a hydroquinone group. The resulting hydroquinone is then oxidized to the corresponding benzoquinone, providing a site for the Diels–Alder mediated immobilization of ligands. The rate constant for the photochemical deprotection is 0.032 s^{-1} (with an intensity of approximately 100 mW/cm^2 between 355 and 375 nm), corresponding to a half-life of 21 s. The hydroquinone is oxidized to the benzoquinone using either electrochemical or chemical oxidation and then functionalized by reaction with a cyclopentadiene-tagged ligand. Two methods for patterning the immobilization of ligands are described. In the first, the substrate is illuminated through a mask to generate a pattern of hydroquinone groups, which are elaborated with ligands. In the second method, an optical microscope fit with a programmable translational stage is used to write patterns of deprotection which are then again elaborated with ligands. This technique is characterized by the use of well-defined chemical reactions to control the regions and densities of ligand immobilization and will be important for a range of applications that require patterned ligands for biospecific interactions.

Introduction

This paper describes a photochemical strategy for generating patterns and gradients of biologically active ligands immobilized to self-assembled monolayers of alkanethiolates on gold. Substrates that are patterned with one or multiple ligands have become important tools in both basic and applied biology.¹ In the former, model substrates that present peptide and carbohydrate ligands are commonly employed as mimics of the extracellular matrix for studies of cell adhesion, migration, and differentiation.² Among the many applications that rely on patterned substrates, the most important are biochips that present arrays of biomolecules and assays for high throughput screening.³ A variety of chemical and physical methods have been developed for preparing the substrates used in each of these settings,⁴ but few methods have the flexibility required to be broadly useful for patterning the surface of SAMs of alkanethiolates on gold. Here we

describe a method—based on the photochemical activation of a benzoquinone group followed by a Diels–Alder mediated immobilization of ligand—that offers wide flexibility in patterning the immobilization of ligands to SAMs.

The methods that have been developed to pattern the immobilization of ligands can be grouped into three classes: photolithographic approaches, contact lithographic approaches, and diffusion-based approaches. The first class of strategies is based on conventional photolithography that illuminates a substrate through a mask to effect photochemical reactions at designated regions of the substrate. By utilizing substrates that react with ligands on illumination with light—or with functional groups that allow the subsequent introduction of ligands—it is possible to pattern the immobilization of ligands at micrometer length scales.⁵ Distefano and co-workers reported one example wherein benzophenone-tagged ligands were covalently immobilized to self-assembled monolayers (SAMs) presenting oligo(ethylene glycol) groups when illuminated at 325 nm.⁶ One difficulty with this and other photochemical methods is a lack of specificity in the immobilization reaction; in this work, for example, repeated insertions of benzophenone groups resulted in oligomerization of ligands at the interface. One important advantage with these photochemical strategies, however, is that they can be combined with an

* To whom correspondence should be addressed. E-mail: mmrksich@uchicago.edu.

[†] Both authors contributed equally to this work.

(1) (a) Park, T. H.; Shuler, M. L. *Biotechnol. Prog.* **2003**, *19*, 243. (b) Jung, D. R.; Kapur, R.; Adams, T.; Giuliano, K. A.; Mrksich, M.; Craighead, H. G.; Taylor, D. L. *Crit. Rev. Biotechnol.* **2001**, *21*, 111. (c) Grebe, T. W.; Stock, *Curr. Biol.* **1998**, *8*, R154. (d) Song, H. J.; Poo, M. M. *Curr. Opin. Neurobiol.* **1999**, *9*, 355. (e) Zicha, D.; Dunn, G. A.; Jones, G. E. *Methods in Molecular Biology*; Pollard, J. W., Walker, J. M., Eds.; Humana Press: Totowa, NJ, 1997; Vol. 75, p 449. (f) Mrksich, M.; Whitesides, G. M. *Trends Biotechnol.* **1995**, *13*, 228.

(2) (a) Kiryushko, D.; Kofoed, T.; Skladchikova, G.; Holm, A.; Berezin, V.; Bock, E. *J. Biol. Chem.* **2003**, *278*, 12325. (b) Kim, J. H.; Glant, T. T.; Lesley, J.; Hyman, R.; Mikecz, K. *Exp. Cell Res.* **2000**, *256*, 445. (c) Clark, P.; Britland, S.; Connolly, P. *J. Cell Sci.* **1993**, *105*, 203. (d) Singhvi, R.; et al. *Science* **1994**, *264*, 696. (e) Clemence, J.-F.; Ranieri, J. P.; Aebischer, P.; Sigrist, H. *Bioconjugate Chem.* **1995**, *6*, 411.

(3) (a) Panda, S.; Sato, T. K.; Hampton, G. M.; Hogenesch, J. B. *Trends Cell Biol.* **2003**, *13*, 151. (b) MacBeath, G.; Schreiber, S. L. *Science* **2000**, *289*, 1760. (c) Delehanty, J. B.; Ligler, F. S. *Anal. Chem.* **2002**, *74*, 5681. (d) Chen, C. S.; Alonso, J. L.; Ostuni, E.; Whitesides, G. M.; Ingber, D. E. *Biochem. Biophys. Res. Commun.* **2003**, *307*, 355. (e) Chiellini, F.; Bizzarri, R.; Ober, C. K.; Schmaljohann, D.; Yu, T.; Solaro, R.; Chiellini, E. *Macromol. Rapid Commun.* **2001**, *22*, 1284.

(4) (a) Lee, K.-B.; Park, S.-J.; Mirkin, C. A.; Smith, J. C.; Mrksich, M. *Science* **2002**, *295*, 1702. (b) Whitesides, G. M.; Ostuni, E.; Takayama, S.; Jiang, X.; Ingber, D. E. *Annu. Rev. Biomed. Eng.* **2001**, *3*, 335. (c) Ziauddin, J.; Sabatini, D. M. *Nature* **2001**, *411*, 107. (d) Delamar, E.; Bernard, A.; Schmid, H.; Michel, B.; Biebuyck, H. *Science* **1997**, *276*, 779.

(5) (a) Wollman, E. W.; Kang, D.; Frisbie, C. D.; Lorkovic, I. M.; Wrighton, M. S. *J. Am. Chem. Soc.* **1994**, *116*, 4395. (b) Tarlov, M. J.; Burgess, D. R. F.; Gillen, G. *J. Am. Chem. Soc.* **1993**, *115*, 5305.

(6) Herbert, C. B.; McLernon, T. L.; Hypolite, C. L.; Adams, D. N.; Pikus, L.; Huang, C.-C.; Fields, G. B.; Letourneau, P. C.; Distefano, M. D.; Hu, W.-S. *Chem. Biol.* **1997**, *4*, 731.

optical microscope and a translational stage to produce patterns and gradients with excellent flexibility and ease.

A second class of strategies for patterning ligands uses contact lithography to deliver ligands and reagents to select regions of a substrate. Microcontact printing—which uses an elastomeric stamp to deliver reagents to planar substrates—has been widely used to pattern SAMs with proteins and ligands.⁷ In one example, contact printing is used to pattern surfaces into regions that alternately promote and resist protein adsorption to give substrates that pattern cell attachment.⁸ In another example, contact printing is used to deliver reactive reagents to a nonpatterned monolayer, which is then treated with a ligand that then immobilizes only on the regions that were contacted by the stamp.⁹ These methods have the advantages that they are experimentally simple, they have excellent resolution (pattern sizes of 1 μm are routine), and they are compatible with a range of substrate materials. These methods, however, are not always well-suited to preparing substrates for biospecific interactions as they are limited by the range of reagents that can be efficiently transferred from stamp to substrate and do not offer strict control over the density of immobilized species. Recently, two additional contact lithography methods have been introduced that use atomic force microscopy (AFM) probes to pattern SAMs at the nanometer regime. The first strategy, nanografting, starts by immersing a SAM in a solution containing an alkanethiol that is different from the one presented on the gold substrate.¹⁰ An AFM tip is used to displace alkanethiolates bound to the gold substrate, and adsorption of new alkanethiols from solution immediately follows. This technique has been used to pattern DNA and proteins at the 10 nm scale.¹¹ The second method—dip-pen nanolithography (DPN)—involves transferring alkanethiols from an AFM tip onto a gold surface, resulting in transfer of the alkanethiols from the probe to the substrate via a solvent meniscus.¹² DPN has been used to pattern a variety of biomolecules with pattern sizes under 100 nm.¹³ These nanolithography methods offer unprecedented control for patterning monolayers at sub-micrometer length scales but can be slow for patterning large areas.

Gradients of immobilized ligands have most commonly been prepared by exposing a substrate to an incompletely mixed solution of reactant or ligand, such that there is a nonuniform concentration of reactant across the substrate. Because the rate of immobilization of the soluble species is related to the concentration of that species, this method results in a gradient density of the immobilized ligand.¹⁴ Spencer and co-workers demonstrated a method based on gradual immersion of a gold-coated substrate into a solution of alkanethiol, leading to a density gradient of

the alkanethiol on the substrate and then treating the substrate with a second alkanethiol to complete formation of the monolayer, giving complementary gradients in each alkanethiolate.¹⁵ Bohn has described another method that uses a nonuniform electrical potential on a substrate to cause desorption of alkanethiolates from a SAM. The SAM is reconstructed by backfilling with a different alkanethiol, resulting in a two-component gradient.¹⁶ These methods allow for coarse control over the geometry of linear or quasi-linear gradients, but they are not well-suited to preparing more complex geometries (i.e., oscillating gradients) or features at length scales below 1 mm.¹⁷ Whitesides and co-workers have made a significant improvement in these methods by constructing gradients using laminar flow of miscible fluids in microfluidic channels. This strategy can control gradients at length scales of 10 μm and further can dynamically adjust the concentration profiles of soluble reagents.¹⁸

The portfolio of methods described above has been important to a range of studies of the properties and effects of patterned and gradient substrates. Our particular interest is in substrates that present peptide and carbohydrate ligands for studies that involve attached cell culture.¹⁹ These substrates pose unique challenges that are not addressed by the methods described above. First, surfaces presenting ligands must be inert to the nonspecific adsorption of protein, to ensure that interactions of cells with the substrate are mediated by the immobilized ligands alone. Second, the densities of immobilized ligands are low (for SAM substrates, between 0.01 and 1% of total alkanethiolate) and must be controlled quantitatively. Finally, the method should allow the sequential patterning of multiple ligands, allowing access to complex substrates. In this paper we describe an approach that is based on the photochemical generation of an immobilized quinone that reacts selectively with diene-tagged ligands. This approach is significant because it uses monolayers that are inert to nonspecific protein adsorption and the rate constants for photodeprotection and Diels–Alder mediated immobilization are uniform, offering excellent control in tailoring substrates with ligands.

Design Rationale

Our approach for patterning the immobilization of ligands begins with SAMs that present nitroveratryloxy-carbonyl (NVOC)-protected hydroquinone groups mixed among a second alkanethiolate. For biologically active substrates, the second alkanethiolate presents an oligo-(ethylene glycol) group because it renders the monolayer inert to the nonspecific adsorption of protein.²⁰ Illumination of the monolayer at 365 nm reveals the hydroquinone, which can then be oxidized to the corresponding benzoquinone using either chemical or electrochemical conversion (and without causing oxidation of the hydroquinone groups that remain protected). The resulting quinone is then reacted with a cyclopentadiene (Cp) conjugate to afford immobilization of the ligand (Figure 1).²¹

(7) Xia, Y.; Whitesides, G. M. *Annu. Rev. Mater. Sci.* **1998**, *28*, 153 and references therein.

(8) (a) Jackman, R. J.; Wilbur, J. L.; Whitesides, G. M. *Science* **1995**, *269*, 664. (b) Mrksich, M.; Dike, L. E.; Tien, J.; Ingber, D. E.; Whitesides, G. M. *Exp. Cell Res.* **1997**, *235*, 305.

(9) Yan, L.; Huck, W. T. S.; Zhao, X.-M.; Whitesides, G. M. *Langmuir* **1999**, *15*, 1208.

(10) Xu, S.; Miller, S.; Laibinis, P. E.; Liu, G.-Y. *Langmuir* **1999**, *15*, 7244.

(11) (a) Jang, C.-H.; Stevens, B. D.; Carlier, P. R.; Calter, M. A.; Ducker, W. A. *J. Am. Chem. Soc.* **2002**, *124*, 12114. (b) Liu, M.; Amro, N. A.; Chow, C. S.; Liu, G.-Y. *Nano Lett.* **2002**, *2*, 863.

(12) Mirkin, C. A. *Inorg. Chem.* **2000**, *39*, 2258.

(13) (a) Lee, K.-B.; Park, S.-J.; Mirkin, C. A.; Smith, J. C.; Mrksich, M. *Science* **2002**, *295*, 1702. (b) Smith, J. C.; Lee, K.-B.; Qian, W.; Finn, M. G.; Johnson, J. E.; Mrksich, M.; Mirkin, C. A. *Nano Lett.* **2003**, *3*, 883.

(14) (a) Pitt, W. G. *J. Colloid Interface Sci.* **1989**, *133*, 223. (b) Lee, J. H.; Kim, H. G.; Khang, G. S.; Lee, H. B.; Jhon, M. S. *J. Colloid Interface Sci.* **1992**, *151*, 563.

(15) Morgenthaler, S.; Lee, S.; Zürcher, S.; Spencer, N. D. *Langmuir* **2003**, *19*, 10459.

(16) Plummer, S. T.; Wang, Q.; Bohn, P. W.; Stockton, R.; Schwartz, M. A. *Langmuir* **2003**, *19*, 7528.

(17) Liedberg, B.; Wirde, M.; Tao, Y.-T.; Tengvall, P.; Gelius, U. *Langmuir* **1997**, *13*, 5329.

(18) Ismagilov, R. F.; Rosmarin, D.; Kenis, P. J. A.; Chiu, D. T.; Zhang, W.; Stone, H. A.; Whitesides, G. M. *Anal. Chem.* **2001**, *73*, 4682.

(19) (a) Mrksich, M. *Curr. Opin. Chem. Biol.* **2002**, *6*, 794. (b) Mrksich, M. *Chem. Soc. Rev.* **2000**, *29*, 267.

(20) Mrksich, M.; Whitesides, G. M. *Annu. Rev. Biophys. Biomol. Struct.* **1996**, *25*, 55.

(21) Yousaf, M. N.; Mrksich, M. *J. Am. Chem. Soc.* **1999**, *121*, 4286.

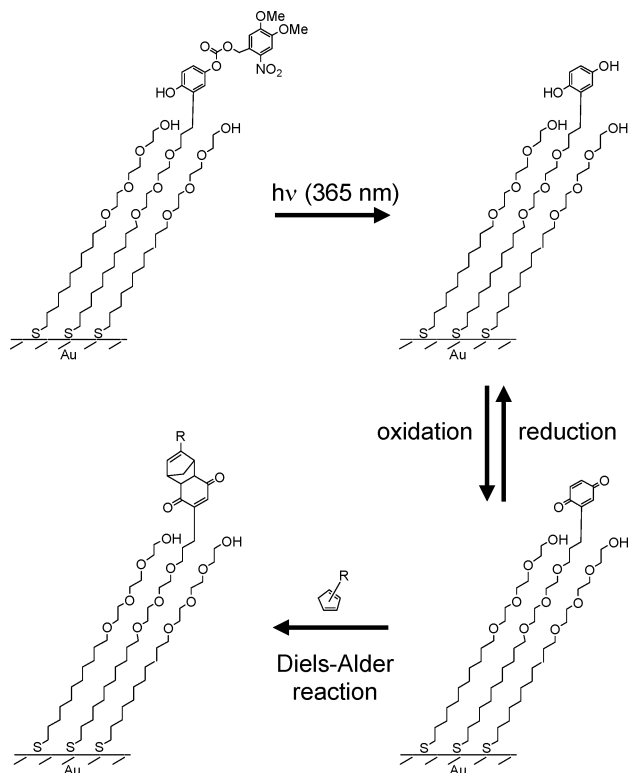


Figure 1. Strategy for patterning the immobilization of ligands to a self-assembled monolayer. A monolayer presenting NVOC-protected hydroquinone is illuminated with ultraviolet light ($h\nu$) at 365 nm to reveal the hydroquinone, which is then reversibly oxidized to the quinone. The quinone undergoes a Diels–Alder reaction with a cyclopentadiene–ligand conjugate to immobilize the ligand. The reversible oxidation of the hydroquinone permits the use of cyclic voltammetry to monitor, in real time, both the photochemical deprotection of the hydroquinone and subsequent Diels–Alder mediated immobilization.

A special feature of these monolayers is that the hydroquinone group undergoes a reversible electrooxidation, which therefore permits the use of cyclic voltammetry to quantitatively monitor the rates for both the photodeprotection and the subsequent Diels–Alder mediated immobilization reactions. This scheme can be adopted to the preparation of patterns and gradients of immobilized ligands either by using photolithographic masks in the illumination or by using a microscope and translational stage to write patterns of deprotection (Figure 2).

Results and Discussion

Synthesis of NVOC-Protected Hydroquinone Alkanethiol (6). The synthesis of the alkanethiol terminated in the NVOC-hydroquinone group is shown in Scheme 1. Hydroquinone was protected as the ditetrahydropyranyl ether **1** and then treated with *tert*-butyllithium and 1,6-dibromohexane to provide the hexyl bromide **2**. Displacement of the bromide with alkoxide **3** afforded the protected hydroquinone-terminated alkanethiol **3**. Deprotection of the two dihydropyranyl ethers under acidic conditions followed by acylation with nitroveratryloxy-carbonyl chloride gave the NVOC derivative **5**. This product was isolated as a mixture of the two regioisomers and used without separation. The trityl protecting group was removed in trifluoroacetic acid to afford the desired alkanethiol **6**.

Preparation of Monolayers. We prepared substrates by electron beam evaporation of titanium (5 nm) and then gold onto either glass cover slips (for patterning experi-

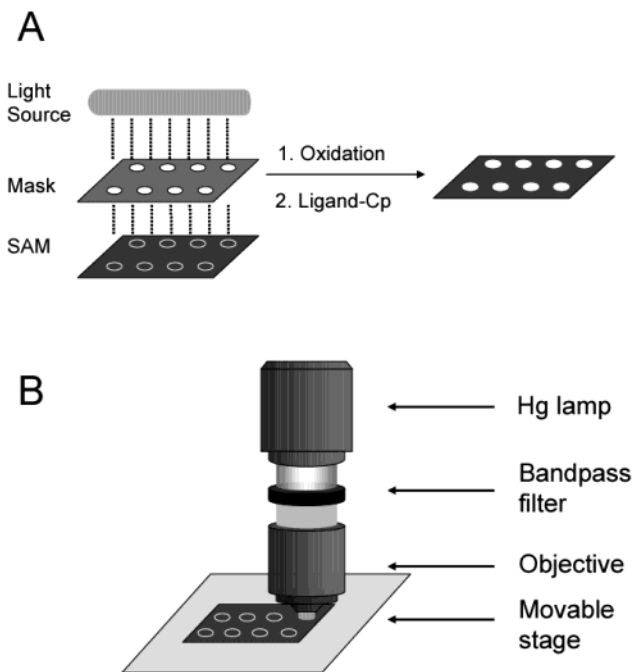


Figure 2. Two strategies for patterning ligands to SAMs. (A) Illumination through a patterned mask reveals the hydroquinone in select regions of the monolayer. Oxidation of the substrate to generate the quinone followed by treatment with a cyclopentadiene–ligand conjugate results in Diels–Alder mediated immobilization of ligand. (B) Schematic for patterning monolayers with scanning lithography. Light from a mercury lamp is filtered through a band-pass filter (355–375 nm) and focused onto a SAM-presenting NVOC-protected hydroquinone. The hydroquinone groups are deprotected by using a movable stage to translate the monolayer in the path of the light using a movable stage.

ments) or silicon wafers (for kinetic studies). Self-assembled monolayers were prepared by immersing the gold-coated substrates into an ethanolic solution containing alkanethiols terminated in the NVOC–hydroquinone group and the tri(ethylene glycol) group (ratio of 19:1, 1 mM total concentration) for 12–16 h and used directly in the experiments described below.

Photochemical Deprotection of NVOC–Hydroquinone. We first characterized the photochemical deprotection of monolayers presenting NVOC-protected hydroquinone groups. We used cyclic voltammetry to quantitatively measure the rate at which the redox-active hydroquinone group was generated. Monolayers were exposed to light from a mercury lamp fit to an optical microscope and filtered through a band-pass filter (355–375 nm) for short periods of time, then cycled between -400 and $+400$ mV (Ag/AgCl reference, 100 mV/s) in a 1:1 mixture of tetrahydrofuran and aqueous phosphate buffer (pH 7.4). We determined the amount of quinone present at the surface by integrating the area under the reduction wave as described previously.²¹ This procedure was repeated several times to obtain a kinetic profile for the deprotection. We fit the data from these experiments to the integrated first-order rate law equation

$$\Gamma_{\text{HQ}} = \Gamma_{\text{PHQ}}^0 (1 - e^{-kt})$$

where Γ_{HQ} is the surface density of hydroquinone, Γ_{PHQ}^0 is the initial surface density of the protected hydroquinone (both with units $\text{mol}\cdot\text{cm}^{-2}$), k is the rate constant for deprotection, and t is total time of illumination in seconds. For the light source used here (approximately 100 mW/

Scheme 1. Synthesis of NVOC-Terminated Alkanethiol

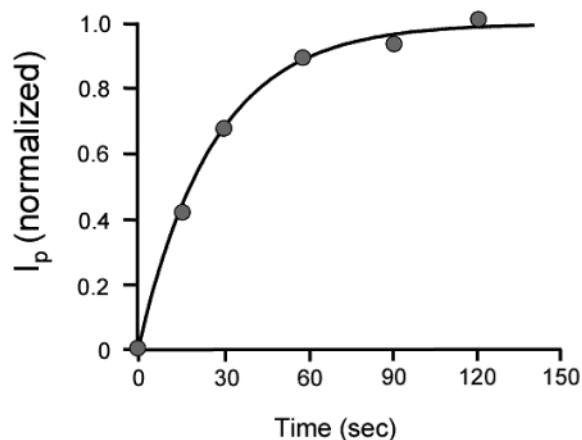
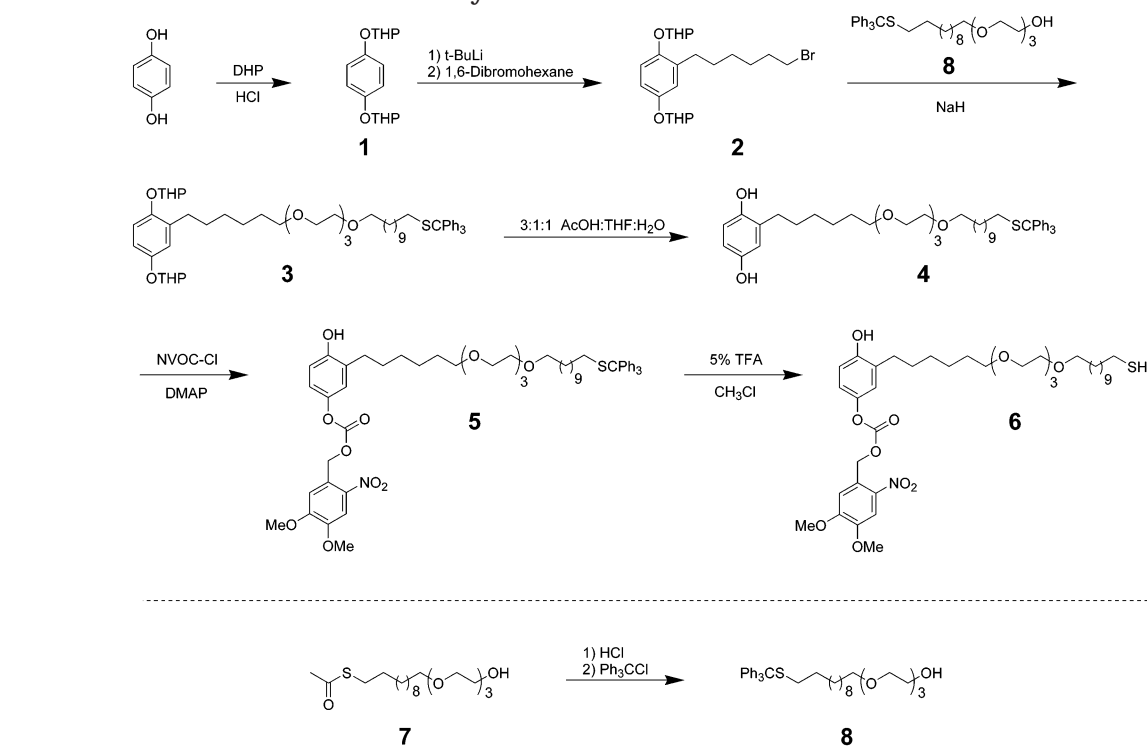
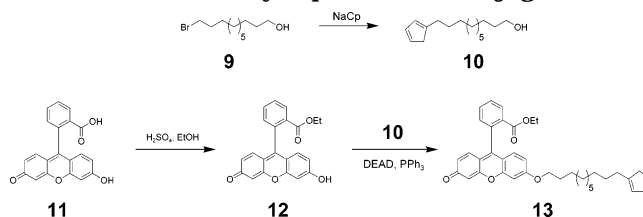


Figure 3. Rate for the photochemical deprotection of self-assembled monolayers presenting NVOC–hydroquinone–alkanethiol (**6**). A plot of the normalized current of the reduction peak (which is proportional to peak area and density of quinone) versus time. The data are fit to the integrated rate law equation (see text for details), giving a rate constant for deprotection of 0.032 s^{-1} and a half-life of approximately 21 s.

cm^2 between 355 and 375 nm), the first-order rate constant for photodeprotection, k , was 0.032 s^{-1} , corresponding to a half-life of 21 s. After 2 min of illumination, cyclic voltammetry showed the deprotection to be essentially complete. Prior to illumination, monolayers showed no redox activity, indicating that all of the hydroquinone groups were protected. Figure 3 shows the amount of deprotection as a function of time of illumination. To verify the presence of hydroquinone groups at the surface, we oxidized the hydroquinone present at the surface by applying a potential of +400 mV (versus Ag/AgCl reference electrode throughout) to the monolayer for 15 s, then reacted the quinone groups with cyclopentadiene. We observed a reaction rate for the interfacial Diels–Alder reaction that was in agreement with that reported earlier ($k_{\text{DA}} \approx 0.24\text{ M}^{-1}\text{ s}^{-1}$).²²

Scheme 2. Synthesis of Fluorescein–Cyclopentadiene Conjugate



Synthesis of Fluorescein–Cp (13**).** We synthesized a conjugate of fluorescein and cyclopentadiene for use in visualizing the patterns resulting from the photochemical patterning of the monolayer (Scheme 2). Substitution of 11-bromo-1-undecanol (**9**) with sodium cyclopentadienide provided 11-cyclopentadienyl-1-undecanol (**10**). Fluorescein **11** was esterified under acidic conditions to give **12** and then coupled to alcohol **10** with a Mitsunobu reaction to afford the fluorescein–cyclopentadiene conjugate **13**.

Photopatterning the Immobilization of Ligands. In a first example, we patterned monolayers by illumination through microfiche masks. Masks were prepared as described by Whitesides and co-workers.²³ Briefly, designs were created using Freehand and printed onto semigloss sheets using an image-setting system with resolution of 3386 dots per inch. The printed images were reduced onto microfiche by a factor of 25. The microfiche masks were placed directly in contact with the monolayer, and exposed to light filtered through a band-pass filter for 2 min. After illumination, the SAM was electrochemically oxidized at +400 mV for 15 s and then treated with F–Cp (20 mM, 30 min) and rinsed. Figure 4 shows fluorescent micrographs for select examples of patterns, prepared using this approach, including a grid of circles, intersecting

(22) Yousaf, M. N.; Chan, E. W. L.; Mrksich, M. *Angew. Chem., Int. Ed.* **2000**, *39*, 1943. (b) Chan, E. W. L.; Yousaf, M. N.; Mrksich, M. *J. Phys. Chem. A* **2000**, *104*, 9315.

(23) Deng, T.; Tien, J.; Xu, B.; Whitesides, G. M. *Langmuir* **1999**, *15*, 6575.

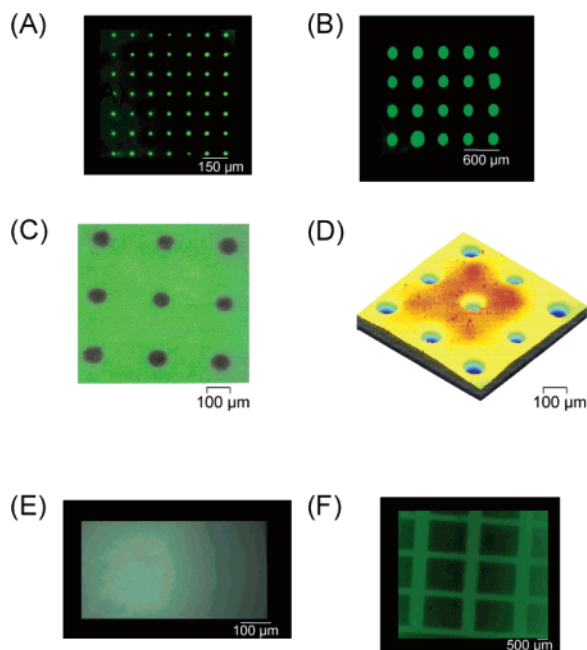


Figure 4. Examples of patterned substrates prepared by illuminating NVOC-protected hydroquinone through microfiche masks. (A) A pattern prepared by illumination through a mask with transparent circles approximately $15\ \mu\text{m}$ in diameter and (B) a pattern formed from a mask with circles approximately $100\ \mu\text{m}$ in diameter. (C) A pattern and (D) intensity profile produced with a negative of the mask used to generate (B). Other examples include (E) a pattern formed using a gradient mask and (F) a pattern formed by sequential illumination through a mask having parallel lines in perpendicular orientations.

perpendicular bars, and a gradient. To obtain fluorescent images, we had to first transfer the monolayer to a transparent polymer. Direct imaging of the substrate gave very weak fluorescence due to quenching by the gold film.²⁴ Instead, poly(dimethylsiloxane) (PDMS) was poured and thermally cured on the SAM. The PDMS was peeled from the SAM—resulting in transfer of the SAM from the gold surface to the PDMS—then imaged using either an optical or confocal microscope.²⁵ Variability in the spot sizes in panels A and B of Figure 4 is most likely due to incomplete contact between the mask and substrate. We observed no immobilization of F-Cp to the SAM (background fluorescence intensity is approximately 10% of observed fluorescence) if the monolayer was oxidized without prior illumination or illuminated without subsequent electrochemical oxidation. These control experiments demonstrate that the NVOC moiety effectively blocks the reversible redox conversion of hydroquinone to quinone and that hydroquinone is generated upon photochemical deprotection.

In a second patterning strategy, we used an optical microscope fitted with a UV light source to pattern the deprotection of SAMs. We used a programmable translational stage to position the substrate in the path of the light at coordinates separated by $2\ \text{mm}$, resulting in a 4 by 4 grid of circles approximately $500\ \mu\text{m}$ in diameter. We used matrix-assisted laser desorption ionization time-of-flight (MALDI-TOF) mass spectrometry to characterize the resulting monolayer and to confirm the geometry of the pattern. Recent work has shown that this technique

is an excellent method for characterizing reactions at SAMs.²⁶ Spectra were acquired in $500 \times 500\ \mu\text{m}$ square regions (the approximate diameter of the laser beam at the surface) on the SAM. We determined the yield of deprotection at each region of the SAM by comparing the intensity of the peaks corresponding to protected and deprotected hydroquinone ($1124.8\ m/z$ and $885.4\ m/z$, respectively).²⁷ Using these results, we constructed a contour plot of the surface by converting the yields of deprotection to a continuous color-coded scale where red represents complete deprotection (i.e., no signal at $1124.8\ m/z$), green represents 50% deprotection, and blue represents no deprotection (Figure 5). The spacing and geometry of deprotection in this image show that photodeprotection of the hydroquinone occurred only in regions exposed to light. It is important to note that each mass spectrum was obtained from a relatively large area. Thus, resolution is somewhat impaired and some deprotected regions of the SAM appear larger than they likely are.

The methodology presented here for patterning ligands to a substrate offers control over two key variables—pattern geometry and density of immobilized adduct. We have shown that masks can be used to control the geometries of a pattern by producing patterns of circles, bars, and gradients. We have demonstrated that the use of a programmable stage allows translational control of the pattern by deprotecting regions of a monolayer exactly $2\ \text{mm}$ apart. Knowledge of the rates of photochemical deprotection and Diels–Alder mediated coupling allows us to control the density of immobilized ligand. With control of pattern geometry and ligand density, we believe that surfaces presenting multiple ligands and two-dimensional gradients can be produced using this methodology and will be important for studying a variety of surface-dependent phenomena, particularly in cell biology.

Patterning Substrates for Attached Cell Culture.

We next demonstrate that this strategy is applicable to preparing substrates for use in experiments involving attached cell culture. This important demonstration establishes that the sequence of steps required to introduce the patterned ligands does not damage the monolayer, which could compromise the inert properties of the substrate and lead to nonspecific attachment of cells. In previous work we showed that monolayers that present the peptide Arg-Gly-Asp support the integrin-mediated attachment and spreading of fibroblast cells.²⁸ The Gly-Arg-Gly-Asp-Ser sequence is known to bind to integrin receptors on the surface of mammalian fibroblast cells and mediate adhesion.²⁹ We prepared a diene-tagged RGD peptide and then patterned the ligand and used the resulting substrates for patterning the attachment of cells.

Synthesis of Peptide–Diene Conjugate (RGD-Cp, 18). Scheme 3 shows the preparation of the peptide–cyclopentadiene conjugate (RGD-Cp, **18**). We used Fmoc-Rink amide MHBA polystyrene as the solid support to synthesize the peptide. We removed the terminal glycyl Fmoc-carbamate with 20% piperidine/DMF, then coupled the peptide with the spacer aminobutyric acid in the presence of DCC and 1-hydroxybenzotriazole (HOBT). We obtained peptide **17** by cleaving the peptide from the resin

(26) Su, J.; Mrksich, M. *Angew. Chem., Int. Ed.* **2002**, *41*, 4715.

(27) As in previous studies, we found that sodium adducts of disulfides are the predominant species observed in MALDI analysis of SAMs. See: (a) Su, J.; Mrksich, M. *Langmuir* **2003**, *19*, 4867. (b) Hanley, L.; Kornienko, O.; Ada, E. T.; Fuoco, E.; Trevor, J. L. *J. Mass Spectrom.* **1999**, *34*, 705.

(28) (a) Yousaf, M. N.; Houseman, B. T.; Mrksich, M. *Angew. Chem., Int. Ed.* **2001**, *40*, 1093. (b) Yousaf, M. N.; Houseman, B. T.; Mrksich, M. *Proc. Natl. Acad. Sci. U.S.A.* **2001**, *98*, 5992.

(29) Ruoslahti, E. *Annu. Rev. Cell Dev. Biol.* **1996**, *12*, 697.

(24) Waldeck, D. H.; Alivisatos, A. P.; Harris, C. B. *Surf. Sci.* **1985**, *158*, 103.

(25) Kumar, A.; Abbott, N. L.; Biebuyck, H.; Kim, E.; Whitesides, G. M. *Acc. Chem. Res.* **1995**, *28*, 219.

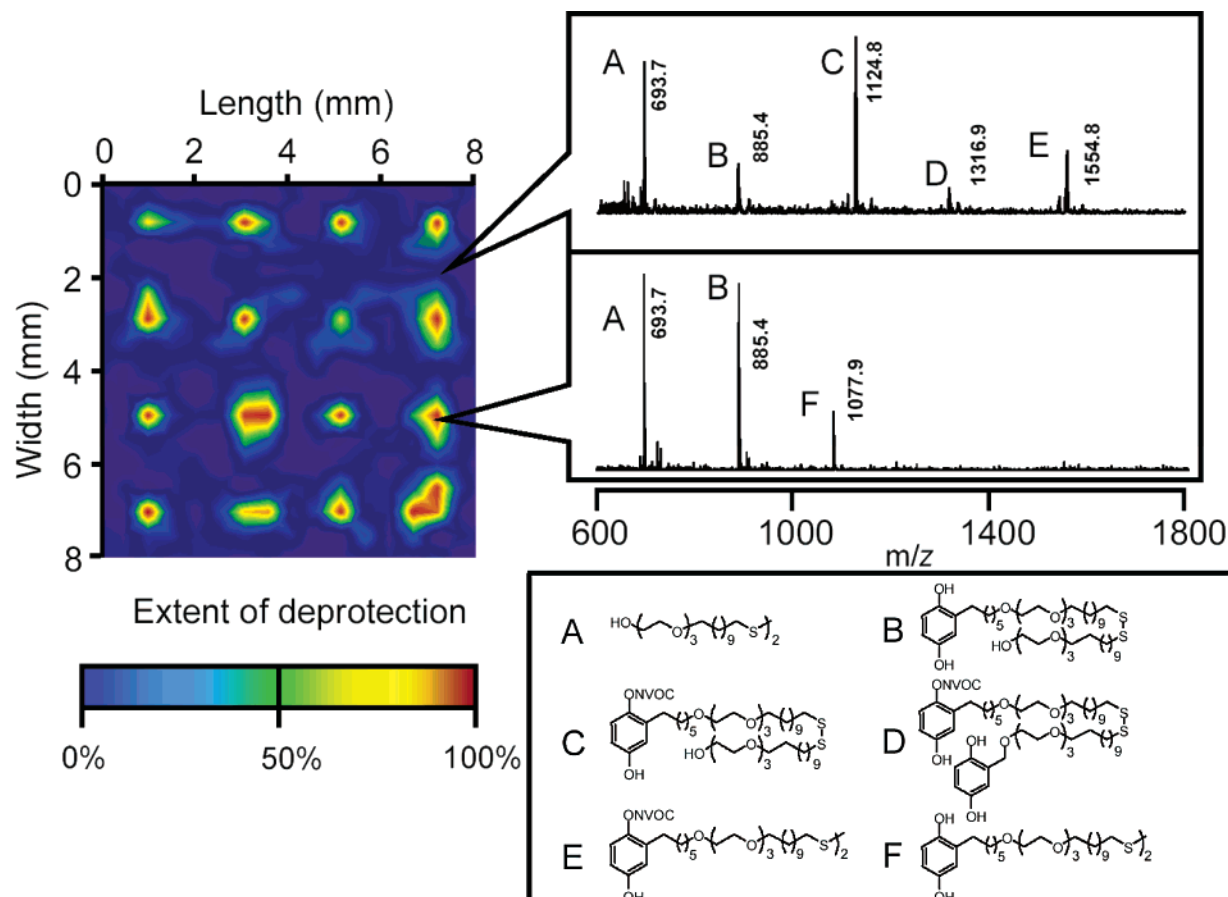
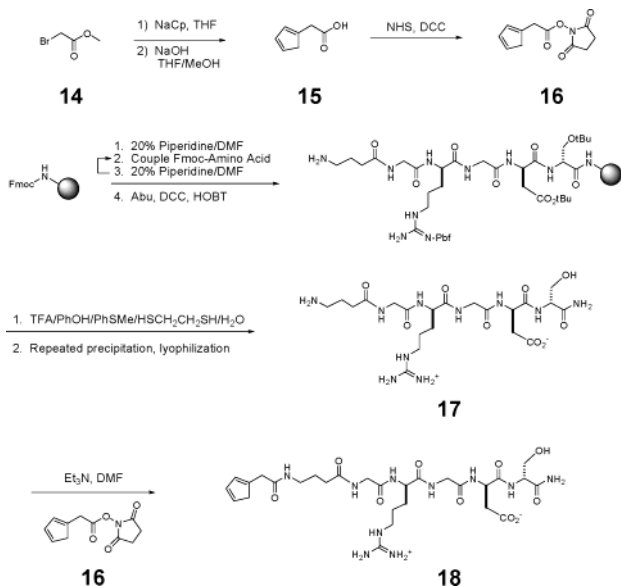


Figure 5. Use of mass spectrometry to spatially characterize a monolayer that was illuminated in an array of circular features. The monolayer was analyzed using MALDI-TOF spectroscopy (see text for details). These data were used to generate a contour plot where the *x*- and *y*-axes are Cartesian coordinates and the *z*-axis is color-coded to signify the extent of deprotection. The spectra specific to two indicated points are shown on the top right with numerical labels indicating the mass-to-charge ratio of each peak. The disulfide corresponding to each peak is letter-coded and shown on the bottom right.

Scheme 3. Synthesis of RGD–Cyclopentadiene Conjugate



and then precipitating repeatedly with ether. Addition of a cyclopentadiene-NHS ester **16** to the peptide generated the RGD-Cp conjugate **18**.

Photopatterning Ligands and Cells to Inert Monolayers. We prepared a SAM by immersing a substrate coated with a layer of gold (15 nm) into a solution of NVOC-protected hydroquinone-terminated alkanethiol **6** and tri-

(ethylene glycol)-terminated alkanethiol (1:99 ratio, 1 mM total thiol) for 10 h. We placed the substrate on a microscope stage, fit it with a microfiche mask, and illuminated the monolayer at 365 nm for 2 min. An electrochemical potential was applied (+400 mV, 15 s) to the substrate to oxidize the deprotected hydroquinone to benzoquinone. We then treated the surface with RGD-Cp (**18**) (5 mM in water, 4 h) to immobilize the peptide via the Diels–Alder reaction. We immersed these substrates in cell culture media, added 3T3 Swiss fibroblasts, and incubated the substrates for 24 h. Fibroblasts attached and spread only on the regions that presented peptide (Figure 6). We confirmed that this interaction is biospecific by blocking adhesion of the fibroblasts to the surface with the addition of soluble GRGDS peptide (1 mM, 1 h). The soluble peptide competes with immobilized RGD for the cell surface integrin receptors, resulting in the detachment of cells from the surface. As further controls, cells did not attach to substrates that were not illuminated, illuminated with no RGD-Cp added, or illuminated with addition of RGD peptide without a cyclopentadiene tether.

Conclusion

The methodology presented here provides a chemically well defined route for patterning ligands to a surface. All of the chemistries involved in this patterning process—photodeprotection, oxidation, and Diels–Alder mediated immobilization of ligands—are kinetically well defined, proceed with high yield, and are accomplished using readily available instrumentation. This combination of

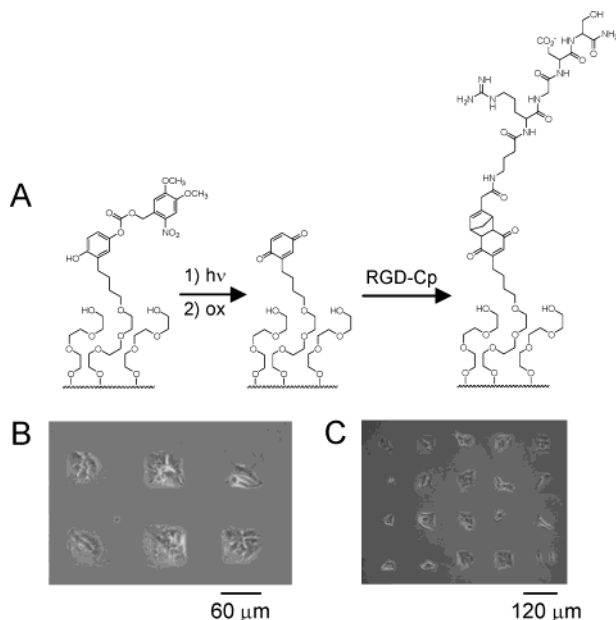


Figure 6. Cells patterned to a self-assembled monolayer by the photodeprotection/Diels–Alder immobilization strategy (see text for details). Swiss 3T3 fibroblasts attach to regions of the substrate that were illuminated with ultraviolet light, oxidized (+400 mV, 15 s), and then treated with RGD-Cp (5 mM, 4 h). The interaction between cell and substrate is specific in that regions not illuminated or illuminated with no RGD-Cp treatment did not support cell attachment.

characteristics allows for the preparation of substrates with excellent control over pattern geometry (including generation of gradients) and the density of immobilized ligand (or multiple ligands). The ability to control these parameters makes this method particularly well suited to fabricating substrates for use in the study of important biological problems—namely, the investigation of cell–cell interactions³⁰ and cell migration.³¹ With advances in optical techniques such as near-field scanning optical microscopy (NSOM),³² it will be possible to immobilize ligands with sub-micrometer precision, enabling the study of cell biology at a scale that is currently difficult.

Experimental Section

All the solvents used for the synthesis were HPLC grade. THF and ethyl ether were distilled from sodium benzophenone ketyl under argon prior to use. Methylene chloride was distilled from calcium hydride. Absolute ethyl alcohol was purchased from Aaper Alcohol Chemical Company. Flash chromatography was carried out using EM science Kieselgel 60 (230–400) mesh. Amino acids and the Fmoc-Rink amide MBHA resin were purchased from Anaspec, Inc. (La Jolla, CA).

All reagents were purchased from Aldrich, Pfaltz & Bauer, and Fluka and used as received.

Confocal Microscopy. The imprinted PDMS was imaged using a Zeiss LSM 510 confocal microscope (Carl Zeiss, Inc., Englewood, CO). The excitation wavelength was 488 nm, and the emission fluorescence was filtered to 505–550 nm. The images were captured and analyzed using a Zeiss LSM 510 image analysis program.

Optical Microscopy. Optical and fluorescent microscopies were performed with an Axiovert 135 microscope. Photographs

were taken on Ilford PanF film (Malelo Camera, Chicago, IL). Digital images were captured and analyzed using NIH imaging software.

Electrochemical Measurements. All electrochemical experiments were performed with a Bioanalytical Systems CV-50W potentiostat using a fabricated cell having a platinum wire as the counter electrode, Ag/AgCl saturated KCl as reference, and the gold/SAM substrate as the working electrode. The cell used a working electrode 0.5 cm² in contact with buffer solution. Substrates were oxidized by applying an oxidative potential of +400 mV for 15 s to convert the hydroquinone groups to quinone groups. All solutions were purged with argon for 30 min before the data acquisition. All experiments were performed at room temperature.

Preparation of Monolayers. The gold substrates were prepared by electron-beam evaporation of an adhesion of titanium (5 nm) and then gold (15 nm for patterning experiments, 100 nm for kinetic experiments) onto a #2 glass cover slip for patterning experiments (Fisher Scientific, Pittsburgh, PA) or a silicon wafer for kinetic experiments (Silicon Sense) in an electron-beam evaporator. The evaporations were performed at a pressure of 2×10^{-7} Torr and a rate of 0.5 nm/s for both metals. The gold-coated substrates were cut into 0.5 cm \times 1.5 cm pieces and washed with absolute ethanol before adsorption of alkanethiols. The monolayers were formed by immersing gold substrates in a solution containing the NVOC-protected hydroquinone-terminated alkanethiol **6** and oligo(ethylene glycol) at an appropriate ratio (1.0 mM thiol concentration) in absolute ethanol at room temperature in a clean scintillation vial for 12–16 h.

Cell Culture. Swiss Albino 3T3 cells (ATCC) were cultured in Dulbecco's Modified Eagle Medium (Gibco) supplemented with 10% fetal bovine serum and penicillin/streptomycin. Cells were removed with a solution of 0.05% trypsin/0.53 mM EDTA, resuspended in serum-free culture medium (60 000 cells/mL), and plated onto the SAM substrates. After 4 h, the serum-free medium was replaced with medium containing serum.

Fabrication of Microfiche Masks. The patterns were designed as Freehand files. The files were printed onto semigloss sheets using an image-setting system with resolution of 3386 dpi by the University of Chicago Printing office. The printed images were then sent to New England Micrographics and optically reduced onto microfiche with 25 \times reduction.

Photochemical Deprotection of Substrates. Substrates were placed on a microscope stage and illuminated through an objective (either 5 \times or 20 \times) with ultraviolet light (AttoArc HBO 100W Hg lamp, Zeiss) filtered through a band-pass filter (365 nm, Coherent, CA) for 2 min (approximately 100 mW/cm²). For experiments in which masks were used, microfiche masks were placed directly in contact with the substrates prior to illumination.

Characterization of Monolayers Using MALDI-MS. Substrates were cut into chips approximately 1 cm² in size. Monolayers were prepared by immersing these chips in a solution containing a 1:1 ratio of NVOC-protected hydroquinone-terminated alkanethiol to tri(ethylene glycol)-terminated alkanethiol (1 mM total alkanethiol concentration in ethanol). Substrates were cleaned and then placed on a microscope stage equipped with a programmable drive (Openlab, Improvion, Lexington, MA) and were deprotected at points 2 mm apart in a 4 by 4 grid for 2 min at each spot. Deprotected substrates were washed with hexanes and ethanol and then dried with a stream of nitrogen. These chips were then treated with acetone containing 2,5-dihydroxybenzoic acid (10 mg/mL, 2 μ L), allowed to dry in air, and then were analyzed on a Voyager-DE Biospectrometry mass spectrometer with a nitrogen laser (337 nm) for desorption and ionization with an accelerating voltage of 20 kV. Molecules were desorbed as disulfide sodium salts. The experimental and calculated mass-to-charge ratio differed by less than 1 amu.

The spectrometer was programmed to analyze the surface by dividing the substrate into regions of squares with sides 500 μ m in length. Four spectra of 75 pulses each were taken within 50 μ m of the center of each region and accumulated. Ions were detected as positive ions on a time-of-flight mass detector in reflector mode. External standards were used for mass calibration. The spectra corresponding to each region of the substrate were then combined to form a contour plot using SigmaPlot software.

(30) (a) Bhatia, S. N.; Balis, U. J.; Yarmush, M. L.; Toner, M. *FASEB J.* **1999**, *13*, 1883. (b) Folch, A.; Jo, B.-H.; Hurtado, O.; Beebe, D. J.; Toner, M. *J. Biomed. Mater. Res.* **2000**, *52*, 346.

(31) (a) Dekker, L. V.; Segal, A. W. *Science* **2000**, *287*, 982. (b) Parent, C. A.; Devreotes, P. N. *Science* **1999**, *284*, 765. (c) Weiner, O. D.; et al. *Nat. Cell Biol.* **1999**, *1*, 75.

(32) Dunn, R. C. *Chem. Rev.* **1999**, *99*, 2891–2927.

Transferring Monolayers from Gold to PDMS. Substrates were placed in tissue culture plates and poly(dimethylsiloxane) (PDMS) was poured onto them (ca. 0.5 mm thick). The tissue culture plate was then placed in an oven (70 °C) for 2 h to cure the polymer. After this time the PDMS was peeled from the tissue culture plate and the gold substrates removed with tweezers. The PDMS was then washed with THF and hexane and dried under a stream of nitrogen. The PDMS was placed on a glass coverslip (0.20 mm, No. 2 Corning) and imaged using confocal or fluorescent microscopy.

11-(Cyclopenta-1,3-dienyl)undecan-1-ol (10). To a solution of 11-bromoundecanol **9** (1.0 g, 4 mmol) in dry THF (20 mL) at 0 °C was added sodium cyclopentadiene (2.4 mL, 2.0 M solution, 4.8 mmol) dropwise over 30 min. The reaction mixture was stirred for 6 h and then diluted with CH₂Cl₂ (30 mL). This solution was then washed 1 × 25 mL of NH₄Cl, 1 × 25 mL of H₂O, 1 × 25 mL of brine, dried over Na₂SO₄, and concentrated to a clear oil. Silica gel chromatography (hexane to 10:1 hexane/ethyl acetate) provided the product as a clear oil (620 mg, 2.62 mmol, 65%). ¹H NMR (400 MHz, CDCl₃): δ 1.25–1.35 (m, 14H), 1.49–1.59 (m, 4H), 2.32–2.41 (m, 2H), 2.86–2.87 (m, 1H), 2.94–2.95 (m, 1H), 3.63 (t, 2H, *J* = 6.8 Hz), 5.98–6.00 (m, 0.5H), 6.14–6.15 (m, 0.5H), 6.23–6.25 (m, 0.5H), 6.41–6.45 (m, 1.5H).

Fluorescein Ethyl Ester (12). To a solution of fluorescein (**11**) (14 g, 42 mmol) in diethylaloxalate (80 mL) was added 10 mL of concentrated H₂SO₄. This reaction mixture was refluxed at 160 °C for 4 h. The reaction mixture was cooled to 0 °C, diluted with 80 mL of a 2:1 CH₂Cl₂/MeOH solution, and then neutralized slowly with saturated NaHCO₃. The reaction mixture was then washed twice with 50 mL of NaHCO₃ and once with 50 mL of brine, dried over Na₂SO₄, and concentrated to a brown solid. The solid was then dissolved in 250 mL of hot ethanol and boiled until the volume was reduced to 60 mL. This solution was then placed in a –20 °C freezer overnight from which red-brown crystals precipitated. The solid was filtered and dried in vacuo. ¹H NMR (400 MHz, DMSO): δ 0.84 (t, 3H, *J* = 7.2 Hz), 3.94 (q, 2H, *J* = 7.2 Hz), 6.55–6.58 (m, 4H), 6.77–6.79 (m, 2H), 7.47–7.49 (m, 1H), 7.75–7.86 (m, 2H), 8.15–8.17 (m, 1H).

Fluorescein–Cyclopentadiene Conjugate (13). To a suspension of fluorescein ethyl ester **12** (500 mg, 1.38 mmol) and triphenylphosphine (545 mg, 2.1 mmol) and alcohol **10** (393 mg, 1.6 mmol) in CH₂Cl₂ (8 mL) was added diethylazodicarboxylate (0.24 mL, 1.5 mmol). The mixture was stirred for 2 h, concentrated in vacuo, and filtered through a pad of silica gel. The filtrate was concentrated to a thick brown oil. Silica gel chromatography (1:1 hexane/ethyl acetate) afforded the conjugate as a red oil (340 mg, 0.57 mmol, 42%). ¹H NMR (400 MHz, CDCl₃): δ 0.95 (t, 3H, *J* = 7.2 Hz), 1.23–1.28 (m, 14H), 1.44–1.46 (m, 4H), 2.33–2.38 (m, 2H), 2.86–2.87 (m, 1H), 2.93–2.94 (m, 1H), 3.99–4.08 (m, 4H), 5.98–5.99 (m, 0.5H), 6.13–6.14 (m, 0.5H), 6.22–6.24 (m, 0.5H), 6.40–6.44 (m, 1.5H), 7.43–7.73 (m, 9H), 8.24–8.26 (m, 1H).

2-(4-(Tetrahydro-2H-pyran-2-yloxy)phenoxy)tetrahydro-2H-pyran (1). To a solution of hydroquinone (2.03 g, 18.4 mmol) in THF (20 mL) was added dihydropyran (8 mL, 86 mmol) and 1 mL of concentrated HCl. This reaction mixture was stirred for 8 h and then diluted with 50 mL of EtOAc. The mixture was washed 3 × 25 mL of NaHCO₃ and 1 × 25 mL of brine, dried over Na₂SO₄, and concentrated to a white solid. Silica gel chromatography (5:1 hexane/ethyl acetate) provided the di-tetrahydropyran hydroquinone as a white solid. ¹H NMR (500 MHz, CDCl₃): δ 1.54–1.65 (m, 6H), 1.80–1.84 (m, 4H), 1.96–1.97 (m, 2H), 3.56–3.59 (m, 2H), 3.88–3.94 (m, 2H), 5.28 (t, 2H, *J* = 4 Hz), 6.96 (s, 4H). ¹³C NMR (CDCl₃): δ 18.89, 25.24, 30.46, 62.03, 97.15, 117.51, 151.87.

2-(2-(Bromohexyl)-4-(tetrahydro-2H-pyran-2-yloxy)phenoxy)tetrahydro-2H-pyran (2). To a solution of 4-(tetrahydro-2H-pyran-2-yloxy)phenoxy)tetrahydro-2H-pyran (**1**) (1.9 g, 6.9 mmol) in dry tetrahydrofuran (20 mL) at 0 °C was added *tert*-butyllithium (4.5 mL of a 1.7 M solution, 7.7 mmol) dropwise over 20 min. This mixture was stirred for 60 min and then brought slowly (over 2 h) to room temperature and stirred for an additional 60 min. To this solution excess 1,6-dibromohexane was added (3.2 mL, 20.7 mmol). A white precipitate was immediately formed, but after stirring for 12 h the solution became clear yellow. The reaction mixture was then diluted with 40 mL of methylene

chloride and washed 1 × 25 mL of NH₄Cl and 1 × 25 mL of brine, dried over Na₂SO₄, and concentrated to a yellow oil. Silica gel chromatography using gradient elution (20:1 hexane/ethyl acetate to 10:1 hexane/ethyl acetate) afforded the product (2.13 g, 5.22 mmol, 75%) as a clear oil. ¹H NMR (500 MHz, CDCl₃): δ 1.62–2.02 (m, 20H), 2.66 (t, 2H, *J* = 7.5 Hz), 3.44 (t, 2H, *J* = 7.8 Hz), 3.58–3.62 (m, 2H), 3.88–3.98 (m, 2H), 5.28–5.32 (m, 2H), 6.84–6.87 (m, 2H), 7.02–7.05 (m, 1H).

2-(2-(2-(11-(Tritylthio)undecyloxy)ethoxy)ethoxy)ethanol (8). To a solution of {1-[(methylcarbonyl)thio]undec-11-yl} tri(ethylene glycol) (**7**)³³ (2.02 g, 5.32 mmol) in absolute ethanol (45 mL) was added concentrated hydrochloric acid (1.7 mL). The reaction solution was refluxed for 16 h, cooled to room temperature, and adjusted to pH 7 with 5% methanolic ammonium hydroxide. The solution was extracted with methylene chloride, dried, and concentrated to an oil. To the crude oil was added dry tetrahydrofuran (40 mL) and triphenylmethyl chloride (2.22 g, 7.98 mmol). The reaction mixture was stirred under nitrogen at room temperature for 18 h and then concentrated. Silica gel chromatography in 1:1 hexanes/ethyl acetate provided the product as a pale yellow oil (1.76 g, 3.04 mmol, 57% over two steps). ¹H NMR (500 MHz, CDCl₃): δ 1.14–1.38 (m, 16H), 1.57 (m, 2H), 2.12 (t, 2H, *J* = 7 Hz), 2.74 (s, 1H), 3.44 (t, 2H, *J* = 6.7 Hz), 3.58–3.71 (m, 12H), 7.16–7.19 (m, 3H), 7.24–7.27 (m, 6H), 7.39–7.41 (m, 6H). ¹³C NMR (CDCl₃): δ 14.16, 21.00, 26.01, 28.52, 28.92, 29.10, 29.32, 29.40, 29.41, 29.48, 29.53, 31.94, 60.32, 61.74, 66.27, 70.02, 70.37, 70.61, 70.64, 71.54, 72.55, 126.42, 127.64, 127.72, 129.52, 129.60, 145.00.

2-(6-(2-(2-(11-(Tritylthio)undecyloxy)ethoxy)ethoxy)ethoxy)hexyl)-4-(tetrahydro-2H-pyran-2-yloxy)phenoxy)-tetrahydro-2H-pyran (3). To a solution of alcohol **8** (2.7 g, 6.7 mmol) in DMF (10 mL) at 0 °C was added NaH (480 mg, 20 mmol) slowly. This reaction mixture was stirred at 0 °C for 1 h and then stirred at room temperature for 2 h. During this time bubbles were observed in the reaction mixture. Bromide **2** (5.45 g, 13.4 mmol) in 5 mL of THF was added dropwise (over 30 min) to the solution. The reaction mixture was stirred for another 5 h at room temperature and then diluted with 40 mL of ethyl acetate. This reaction mixture was then washed with 1 × 25 mL of NH₄Cl 1 × 25 mL of brine, dried over Na₂SO₄, and concentrated to a yellow oil. Silica gel chromatography (1:9 ethyl acetate/hexanes to 100% ethyl acetate) afforded the product as a clear oil (1.91 g, 3.82 mmol, 57%). ¹H NMR (500 MHz, CDCl₃): δ 1.19–1.40 (m, 20H), 1.59–1.68 (m, 10H), 1.83–1.87 (m, 4H), 2.15 (t, 2H, *J* = 6.8 Hz), 2.65 (t, 2H, *J* = 7.0 Hz), 3.44–3.51 (m, 4H), 3.58–3.67 (m, 16H), 3.92–3.95 (m, 2H), 5.30–5.2 (m, 2H), 6.84–6.88 (m, 2H), 6.99 (d, 1H, *J* = 8.5 Hz), 7.20 (t, 3H, *J* = 7.2 Hz), 7.26 (m, 6H, *J* = 7.2 Hz), 7.44 (d, 6H, *J* = 7.2 Hz). ¹³C NMR (CDCl₃): δ 18.81, 18.87, 25.17, 25.22, 25.90, 25.97, 28.46, 28.88, 29.05, 29.28, 29.33, 29.36, 29.43, 29.51, 29.52, 29.99, 30.40, 30.44, 30.59, 31.88, 61.77, 61.86, 69.95, 70.50, 71.38, 71.39, 96.69, 96.94, 114.24, 115.12, 118.33, 126.36, 127.66, 129.47, 132.77, 144.95, 149.73, 151.33. LRMS (FAB): calculated for C₅₆H₇₈O₈S (MH⁺) *m/e* 910.54, found *m/e* 910.60.

2-(6-(2-(2-(11-(Tritylthio)undecyloxy)ethoxy)ethoxy)ethoxy)hexyl)benzene-1,4-diol (4). Oil **3** (900 mg, 0.958 mmol) was taken up in 40 mL of a 3:1 mixture of acetic acid/water/tetrahydrofuran and stirred for 16 h. The reaction mixture was concentrated, taken up in ethyl acetate, and washed twice with 0.01 M NaOH. The organic layer was dried and evaporated, affording the product (715 mg, 0.890 mmol, 93%). ¹H NMR (500 MHz, CDCl₃): δ 1.19–1.39 (m, 18H), 1.59–1.68 (m, 8H), 2.10 (t, 2H, *J* = 6.8 Hz), 2.54 (t, 2H, *J* = 7.5 Hz), 3.39–3.42 (m, 4H), 3.54–3.65 (m, 12H), 4.69 (s, 1H), 5.06 (s, 1H), 6.51 (dd, 1H, *J* = 8.8 Hz, 3.2 Hz), 6.60–6.62 (m, 2H), 7.18 (t, 3H, *J* = 7.2 Hz), 7.25 (m, 6H, *J* = 7.2 Hz), 7.42 (d, 6H, *J* = 7.2 Hz).

2-(6-(2-(2-(11-(Tritylthio)undecyloxy)ethoxy)ethoxy)ethoxy)hexyl)-4-hydroxyphenyl 4,5-Dimethoxy-2-nitrobenzylcarbonate (5). To a solution of **4** (155 mg, 0.201 mmol) in dry methylene chloride (10 mL) was added 4-(dimethylamino)pyridine (37 mg, 0.30 mmol) and 4,5-dimethoxy-2-nitrobenzyl chloroformate (69 mg, 0.25 mmol). This reaction mixture was stirred under nitrogen for 12 h at room temperature. The mixture

(33) Pale-Grosdemange, C.; Simon, E. S.; Prime, K. L.; Whitesides, G. M. *J. Am. Chem. Soc.* **1991**, *113*, 12.

was diluted with 25 mL of methylene chloride, then washed twice with 0.1 M HCl, and dried over MgSO₄. The organic layer was concentrated to a yellow oil. Silica gel chromatography (3:1 hexanes/ethyl acetate to 1:1 hexanes/ethyl acetate) afforded mixed isomers of the product as a clear yellow oil (77 mg, 0.076 mmol, 38%). ¹H NMR (500 MHz, CDCl₃): δ 1.18–1.37 (m, 18H), 1.58–1.67 (m, 8H), 2.09 (t, 2H, *J* = 6.8 Hz), 2.52 (t, 2H, *J* = 7.5 Hz), 3.36–3.42 (m, 4H), 3.49–3.60 (m, 12H), 3.95 (s, 3H), 3.98 (s, 3H), 5.62 (s, 2H), 6.01 (s, 1H), 6.69 (d, 1H, *J* = 8.0 Hz), 6.77–6.84 (m, 2H), 7.08 (s, 1H), 7.18 (t, 3H, *J* = 7.2 Hz), 7.25 (m, 6H, *J* = 7.2 Hz), 7.42 (d, 6H, *J* = 7.2 Hz), 7.72 (s, 1H).

2-(6-(2-(2-(11-Mercaptoundecyloxy)ethoxy)ethoxy)hexyl)-4-hydroxyphenyl 4,5-Dimethoxy-2-nitrobenzylcarbonate (6). To a solution of carbonate **5** (31 mg, 0.031 mmol) in 5% trifluoroacetic acid in methylene chloride (5 mL) was added triethylsilane (0.025 mL, 0.155 mmol). The reaction mixture was stirred under nitrogen for 10 h and then concentrated to a yellow oil. Silica gel chromatography (6:1 hexanes/ethyl acetate to 1:1 hexanes/ethyl acetate) afforded the product as a clear oil (22 mg, 0.029 mmol, 93%). ¹H NMR (400 MHz, CDCl₃): δ 1.23–1.37 (m, 18H), 1.52–1.61 (m, 8H), 2.49 (quartet, 2H, *J* = 7.3 Hz), 2.57 (t, 2H, *J* = 7.4 Hz), 3.39–3.44 (m, 4H), 3.53–3.64 (m, 12H), 3.95 (s, 3H), 3.98 (s, 3H), 5.65 (s, 2H), 6.10 (broad s, 1H), 6.73 (d, 1H, *J* = 8.6 Hz), 6.83 (dd, 1H, *J* = 8.6 Hz, 2.8 Hz), 6.90 (d, 1H, *J* = 2.8 Hz), 7.10 (s, 1H), 7.74 (s, 1H). LRMS (FAB): calculated for C₃₉H₆₁NO₁₂S (M⁺H – CO₂) calculated *m/e* 724.4, found *m/e* 724.3.

2-(Cyclopenta-1,3-dienyl)acetic Acid (15). To a solution of bromide **14** (2.45 g, 17.8 mmol) in dry THF (50 mL) at 0 °C was added sodium cyclopentadiene (10.7 mL, 2.0 M solution, 21.4 mmol) dropwise over 90 min. The reaction mixture was stirred for 6 h and then diluted with CH₂Cl₂ (60 mL). This solution was then washed 1 × 50 mL of NH₄Cl, 1 × 50 mL of H₂O, and 1 × 50 mL of brine, dried over Na₂SO₄, and concentrated. The resulting crude ester was taken up in THF/MeOH (2:1, 120 mL), and to this solution was added 1 N NaOH (36.5 mL). The solution was stirred at room temperature for 3 h and concentrated to a volume of 50 mL. Dichloromethane (100 mL) was added, and the aqueous phase was acidified to a pH of 2 with 1 N HCl. The aqueous phase was extracted once with dichloromethane (25 mL), and the combined organic phases were washed with H₂O (25 mL) and brine (25 mL). The organic layer was dried with sodium sulfate, filtered, and concentrated to provide a yellow solid. ¹H NMR (400 MHz, CDCl₃): δ 3.01–3.04 (m, 2H), 3.46–3.49 (m, 2H), 6.25–6.52 (m, 3H).

2-(Cyclopenta-1,3-dienyl)aceto-*N*-hydroxysuccinimide (16). To a solution of the acid **15** (310 mg, 2.5 mmol) in THF (15 mL) was added NHS (300 mg, 2.5 mmol) and DCC (510 mg, 2.55 mmol). A white precipitate formed immediately. After 4 h, the reaction mixture was filtered through a pad of Celite and concentrated to a yellow oil. Silica gel chromatography (CH₂Cl₂ to 30:1 CH₂Cl₂/EtOAc) provided the activated ester as a clear oil (200 mg, 70%): ¹H NMR (500 MHz, CDCl₃): δ 2.81 (s, 4H), 3.02 (m, 1H), 3.07 (m, 1H), 3.70 (m, 1H), 3.73 (m, 1H), 6.35–6.53 (m,

3H). ¹³C NMR (CDCl₃): δ 25.5, 32.2, 33.0, 41.7, 43.4, 131.1, 131.8, 132.0, 133.3, 133.4, 134.7, 136.0, 136.7, 166.3, 169.0.

Solid-Phase Peptide Synthesis. Fmoc-Rink amide MBHA resin (312 mg, 0.15 mmol, substitution 0.48 mmol/g) was placed in a 10 mL polypropylene reaction vessel, washed with DMF (2 × 5 mL), and swollen for 30 min in DMF. The resin was rinsed with an additional portion of DMF before a solution of 20% piperidine in DMF (5 mL, 2 × 15 min) was added. The resin was washed with DMF (2 × 5 mL) before a solution of the Fmoc-amino acid (0.45 mmol), HOBT (68 mg, 0.5 mmol), and DCC (95 mg, 0.46 mmol) in DMF (5 mL) was added to the vessel. The mixture was agitated for 2 h, at which point the Kaiser ninhydrin test was negative. The deprotection and coupling cycles were repeated until assembly of the Fmoc-protected Abu-Gly-Arg-Gly-Asp-Ser peptide was complete. To cleave the peptide, the resin was placed in a 25 mL round-bottomed flask, and a solution of 5 mL of TFA containing 0.25 mL of H₂O, 0.375 g of phenol, 0.25 mL of ethanedithiol, and 0.25 mL of thioanisole was added. The yellow mixture was stirred at room temperature for 2 h and filtered to remove the polymeric support. The beads were washed with TFA (2 × 2 mL), and the combined filtrates were concentrated in vacuo. Repeated precipitation from cold ether (4 × 40 mL) and centrifugation afforded a white solid that was lyophilized to afford the peptide as a fluffy, white powder (88 mg, 58% based on loading of resin).

2-(Cyclopenta-1,3-dienyl)aceto-Gly-Arg-Gly-Asp-Ser (18). To a solution of the peptide **17** (490 mg, 1 mmol) in DMF (4 mL) was added triethylamine (2.1 mmol). The solution was stirred for 2 min before a solution of activated ester **16** (200 mg, 1.02 mmol) in DMF (2 mL) was added. The reaction mixture was stirred at room temperature for 2 h. The reaction mixture was added dropwise to 100 mL of cold ether to afford a white precipitate. The precipitate was collected by centrifugation and washed sequentially with THF (2 × 50 mL), CH₂Cl₂ (50 mL), THF (2 × 50 mL), and ether (50 mL). Lyophilization of the precipitate provided peptide–cyclopentadiene conjugate as a fluffy white solid that could be used without further purification. An analytical sample was prepared using RP-HPLC (C₁₈ column, 0–10% CH₃CN:H₂O *without* TFA). ¹H NMR (500 MHz, CDCl₃): δ 1.66–1.95 (m, 10H), 2.82–2.88 (m, 1H), 3.00–3.06 (m, 4H), 3.21 (t, 2H, *J* = 7.0 Hz), 3.29–3.31 (m, 1H), 3.46–3.49 (m, 2H), 3.75–3.90 (m, 4H), 4.33 (t, 1H, *J* = 7.0 Hz), 4.38 (t, 1H, *J* = 5.0 Hz), 4.72 (t, 1H, *J* = 6.5 Hz), 6.25–6.52 (m, 3H). ¹³C NMR (CDCl₃): δ 26.02, 28.56, 28.97, 29.13, 29.35, 29.42, 29.45, 29.50, 29.55, 31.99, 66.32, 68.92, 69.98, 70.34, 70.42, 70.45, 70.49, 70.52, 70.54, 70.61, 70.65, 71.32, 71.50, 126.44, 127.74, 129.57, 145.05, 171.95. IR (thin film): 3057, 2916, 2852, 1735. HRMS (FAB): calcd for C₄₄H₆₄O₉SK (M + K⁺) 807.3908, found 807.3909.

Acknowledgment. This work was supported by the National Science Foundation and the National Institutes of Health.

LA049826V